Microscopic model of charge-density waves in $2H$-$TaSe_2$†

W. L. McMillan

Department of Physics and Materials Research Laboratory, University of Illinois at Urbana-Champaign, Urbana, Illinois 61801

(Received 16 September 1976)

A microscopic model of charge-density waves in $2H$-$TaSe_2$ at zero temperature is developed and applied to calculate the lattice dynamics in the commensurate phase. The results are compared with the Raman data of Holy *et al.* At finite temperatures the conventional microscopic approach is to assume that the important excitons are electrons excited across the Peierls gap in the band structure. This conventional theory leads to gross inconsistencies in attempting to fit the experimental data for $2H$-$TaSe_2$. The theory is reformulated, assuming that the coherence length is very short and that the dominant entropy is the lattice entropy. The lattice-entropy model is in good agreement with experiment at the semiquantitative level; the quantitative discrepancies appear to be due in part to the neglect of critical fluctuation effects.

I. INTRODUCTION

Our present understanding of charge-density waves (CDW) in metals follows from the early work of Peierls,[1] Fröhlich,[2] Overhauser,[3] and Chan and Heine.[4] In the past two years there has been an extensive experimental study of CDW's in one-dimensional organic materials [e.g., (tetrathiafulvalene-tetracyanoquinodimethane) TTF-TCNQ][5] and the transition-metal dichalogenides[6] (e.g., $2H$-$TaSe_2$). There is now sufficient experimental data for one material, $2H$-$TaSe_2$, to quantitatively test the microscopic models that have been proposed.

The Peierls model and most of the subsequent theoretical work is based on the following physical picture: One starts with a normal metal and introduces a periodic lattice distortion (a static phonon distortion of finite amplitude and wave vector $\vec{q}$). The lattice distortion creates a band gap in the one-electron band structure. If the wave vector $\vec{q}$ spans nested portions of the Fermi surface, the energy of many occupied electronic states will decrease and the total electronic energy will decrease. If the gain in electronic energy more than offsets the increase in elastic energy the distorted state will be the ground state. The occupied electronic states are nonuniform and there is a CDW with wave vector $\vec{q}$ which screens the lattice potential. Thus, the three physical properties go together, the periodic lattice distortion, the energy gap in the band structure, and the CDW. I believe that this physical picture is correct for $2H$-$TaSe_2$ and do not challenge it in this paper. However, in order to calculate the properties of the CDW state at finite temperature the conventional approach is to include the entropy of electrons excited across the energy gap. This approach predicts an energy gap at zero temperature $2W_0 \simeq 3.5\ kT_{IN}$, where T_{IN} is the incommensurate to normal-state transition temperature, and a BCS-like temperature dependence of the energy gap. This approach should be correct if the coherence length ξ_0 is long; however it leads to gross inconsistencies in attempting to fit the experimental data for $2H$-$TaSe_2$ as we show in Sec. IV.

In Sec. V, we reformulate the microscopic theory at finite temperatures assuming that the coherence length is short and that the phonon entropy rather than the electronic entropy is important. This short coherence-length model is in good agreement with the available experiments. We find a coherence length $\simeq 3.5$ Å and an energy gap $\simeq 30\ kT_{IN}$ which agrees with the infrared gap observed by Barker *et al.*

We conclude with a few remarks on the relationship between charge-density waves and chemical bonding.

II. THEORETICAL MODEL AT $T = 0$

We adopt a simplified theoretical model of CDW's in a metal similar to that used by Bilbro and McMillan.[7] We write the displacement of the ith Ta atom in the lth layer from its lattice site $\vec{R}_i$ as

$$\vec{u}_l(\vec{R}_i) = \mathrm{Im}\sum_{j=1}^{3} \hat{q}_j \phi_i^j(R_i) e^{i\vec{q}_j \cdot \vec{R}_i} , \tag{1}$$

where $\vec{q}_j$ is the nesting vector of the jth CDW and $\phi_i^j(\vec{R}_i)$ is the local complex amplitude of the CDW. The three $\vec{q}_i$ form a star in the ΓM directions. According to the Chan and Heine model the screening of the electron-phonon interaction is temperature dependent in the normal state and temperature independent in the CDW state. We neglect the temperature and q dependence of the electron-phonon coupling constant α and write

$$W_i^j(x) = \alpha \phi_i^j(x) , \tag{2}$$

where $2|W_i^j(x)|$ is the local energy gap in the one-electron band structure due to the lattice distor-

tion. Only a portion of the Fermi surface will be affected by the energy gap W_l^j and we assume a simplified band structure for this nested portion: we assume perfect nesting with a Fermi velocity v_F and an electronic density of states (of one spin) of $N_\uparrow(0)$ (for each CDW). Then the electronic energy is easily shown to be

$$E_{el}=\sum_{lj}\int d^2x\left(-N_\uparrow(0)|W_l^j(x)|^2\ln\frac{E_B^2}{|W_l^j(x)|^2}+N_\uparrow(0)\xi_0^2|\nabla W_l^j(x)|^2\right), \tag{3}$$

where E_B is the electronic band width and ξ_0 is the correlation length which is of order $\hbar v_F/2W$. We have taken a correlation length which is isotropic in the plane even though an anisotropic correlation length is permitted by symmetry. Electrons near the gap edge cannot respond to lattice vibrations with wave vectors further than $1/\xi_0$ from the nesting vector and we assume that $\phi_l^j(x)$ is a slowly varying function with momentum space cutoff of $k_c=1/\xi_0$. The number of phonon modes which participate in the CDW phase transition is limited by this physical cutoff.

There are several other energies which are important in this problem; we will first write down the complete energy expression and then discuss the individual terms. Since we will deal primarily with phonon frequencies we will use ϕ instead of W as a variable. The total (potential) energy is

$$E_P=\frac{1}{2}\sum_l\int\frac{d^2x}{\Omega}\left(\sum_j\left[A|\phi_l^j|^2-C|\phi_l^j|^2\ln|\phi_B/\phi_l^j|^2+C\xi_0^2|\nabla\phi_l^j|^2-\mathrm{Re}(B_l\phi_l^{j\,3}e^{i(3\vec{q}_j-\vec{G})\cdot\vec{x}})+F\,\mathrm{Re}(\phi_l^j\phi_{l+1}^j)\right]\right.$$
$$\left.+D(|\phi_l^1\phi_l^2|^2+|\phi_l^1\phi_l^3|^2+|\phi_l^2\phi_l^3|^2)+\mathrm{Re}(E\phi_l^1\phi_l^2\phi_l^3)\right), \tag{4}$$

where Ω is the area of the normal-state unit cell in one plane, and B and E are complex constants. The first term in the energy is the unscreened elastic constant, and the second and third terms are the electronic contributions from (3). The fourth term is the lock-in term; it contributes only when the wavelength of the CDW is three times the lattice spacing. The fifth term is the interlayer interaction due to Coulomb and Van der Waals interactions. The sixth term is a CDW interaction which arises when two CDW's compete to open an energy gap on the same portion of Fermi surface. Finally, the seventh term is a weak CDW interaction permitted by symmetry.

The lattice kinetic energy is

$$E_K=\frac{M^*}{4}\sum_{lj}\int\frac{d^2x}{\Omega}\left|\frac{\partial\phi_l^j(x)}{\partial t}\right|^2, \tag{5}$$

where the Se atoms are assumed to adiabatically follow the Ta atoms and with the same ratio of Se displacement to Ta displacement as observed at low temperature[8]; this yields $M^*=206$ au. Equations (4) and (5) constitute a dynamical model for the longitudinal-acoustic-phonon modes near $\vec{q}_j$.

III. LATTICE DYNAMICS AT $T=0$

At $T=0$ in the commensurate phase the equilibrium state is found by setting

$$\phi_l^j(x)=\phi_0 e^{i(\theta_l+\Delta\vec{q}\cdot\vec{x})}, \tag{6}$$

where $\Delta\vec{q}=\frac{1}{3}\vec{G}_j-\vec{q}_j$. The lock-in energy dominates in fixing the phase θ_l of the CDW. With the origin of coordinates at the inversion center (midway between planes and above a Ta atom) we have $B_l^*=B_{l+1}$ and

$$\theta_l=-\tfrac{1}{3}\theta(B_l), \tag{7}$$

where $\theta(B_l)$ is the phase of B_l. Then minimizing the energy with respect to ϕ_0 we find

$$A+C\xi_0^2\Delta q^2-C\ln(\phi_B/\phi_0)^2+C-\tfrac{3}{2}|B|\phi_0+2D\phi_0^2+\tfrac{1}{2}\mathrm{Re}(Ee^{i3\theta_0}\phi_0)-F=0, \tag{8}$$

which determines ϕ_0.

In order to find the phonon frequencies we add a small phase or amplitude distortion to the static distortion

$$\phi_l^j(\vec{x})=[\phi_0+(\alpha_k+i\beta_k)\cos(\vec{k}\cdot\vec{x}+\tfrac{1}{2}k_z lc)]e^{i\theta_l+i\Delta\vec{q}\cdot\vec{x}} \tag{9}$$

and expand the potential energy to second order in α_k and β_k. For the amplitude modes we find

$$\tfrac{1}{4}M^*\omega_k^2=4C-3|B|\phi_0+8D\phi_0^2+\overline{E}\phi_0+2F-2F\cos(\tfrac{1}{2}k_z c)+C\xi_0^2k^2 \tag{10a}$$

and

$$\tfrac{1}{4}M^*\omega_k^2=4C-3|B|\phi_0-4D\phi_0^2-2\overline{E}\phi_0+2F-2F\cos(\tfrac{1}{2}k_z c)+C\xi_0^2k^2, \tag{10b}$$

where $\overline{E}=\mathrm{Re}[E\exp(i3\theta_0)]$. For the phase modes we find

$$\tfrac{1}{4}M^*\omega_k^2=9|B|\phi_0-3\overline{E}\phi_0+2F-2F\cos(\tfrac{1}{2}k_z c)+C\xi_0^2k^2 \tag{10c}$$

and

$$\tfrac{1}{4}M^*\omega_k^2 = 9|B|\phi_0 + 2F - 2F\cos(\tfrac{1}{2}k_z c) + C\xi_0^2 k^2 . \tag{10d}$$

The (10b) and (10d) modes are doubly degenerate giving six modes. These modes are formed from the star of six longitudinal-acoustic modes at $\pm(\vec{q}_j + \Delta\vec{q})$, $j = 1, 2, 3$ which are mapped back into the origin of reciprocal space by the CDW. Note that since the unit cell is two layers in the c direction, wave vectors $\vec{k} = 0$, $k_z = 0$ and $\vec{k} = 0$, $k_z = \pi/c$ appear at Γ so that there are twelve modes at Γ, six from each of two layers. The symmetries of these modes were given in Ref. (9). From the Raman data[9] the following parameters were determined:

$$F \simeq 0.03 \text{ eV/Å}^2; \quad |B|\phi_0 = 0.053 \text{ eV/Å}^2;$$

$$|E\phi_0| = 0.036 \text{ eV/Å}^2;$$

$$C = 0.29 \text{ eV/Å}^2, \quad D\phi_0^2 = 0.031 \text{ eV/Å}^2;$$

$$A/C + \xi_0^2\Delta q^2 - \ln|\phi_B/\phi_0|^2 = -0.90.$$

IV. CONVENTIONAL THEORY AT FINITE T

There is now sufficient experimental data on 2H-$TaSe_2$ to provide a quantitative test of theoretical models of charge-density waves. Susceptibility, resistivity, and transition temperatures are available from Wilson, DiSalvo, and Mahajan[6] and a complete neutron crystallographic study has been performed by Moncton and Axe.[8] Barker *et al.*,[10] have observed an energy gap of 0.25 eV, which they interpret as the CDW energy gap. Recently, Craven[11] has measured the heat capacity near the phase transition using the high-resolution ac technique and Klein's group[9] have measured and interpreted the Raman spectrum. Thus we have the opportunity, for the first time, to find out whether the theoretical models really work for real materials. We first examine the "conventional theory" and find that it fails badly at finite temperatures.

If the ideas of Sec. II are correct, we have only to add the appropriate entropy term to do the theory at finite temperature. If the coherence length is long (compared with the lattice spacing or the interelectron spacing), the phonon frequencies are modified only over a small region of reciprocal space and the phonon entropy is unimportant. The important entropy is that of electrons excited across the energy gap in the band structure. Note that for long coherence lengths, critical fluctuations are unimportant and mean-field theory is exact. We wish to calculate the transition temperature and the heat-capacity jump at the incommensurate–normal-state transition. The lock-in energy does not contribute and the interlayer and cubic terms in Eq. (4) are small enough to be neglected. The CDW interaction term (with coefficient D) is large enough to be important; however it does not affect the transition temperature and it reduces the heat-capacity jump which, as we shall see, increases the discrepancy between theory and experiment. Since that discrepancy is large enough to be convincing already, for our present purposes we can omit the CDW interaction term also. Thus the only important energies are the band-structure energy (3) and the quadratic lattice energy. We assume a perfectly nested Fermi surface for each CDW and write for the energy bands in the normal state

$$E_{\vec{k}}^{\pm} = hv_F|k_x \pm \tfrac{1}{2}q| . \tag{11}$$

In the presence of a static lattice distortion the energy bands are

$$E_{\vec{k}}^{\pm} = \pm(h^2v_F^2|k_x - \tfrac{1}{2}q|^2 + W^2)^{1/2} \tag{12}$$

and the total energy per unit volume per CDW is

$$E = 2\sum_{\vec{k}}(E_{\vec{k}}^{+}n_k^{+} + E_k^{-}n_k^{-}) + \frac{N_{Ta}A}{2\alpha^2}W^2 , \tag{13}$$

where $n_k^{\pm}$ is the occupation probability of the $\vec{k}^{\pm}$ band state and N_{Ta} is the density of Ta atoms. The electronic entropy is

$$S = 2\sum_k [n_k^{+}\ln n_k^{+} + (1-n_k^{+})\ln(1-n_k^{+}) + n_k^{-}\ln n_k^{-} + (1-n_k^{-})\ln(1-n_k^{-})] . \tag{14}$$

Minimizing the free energy $F = E - TS$ with respect to $n_k^{\pm}$ we find

$$n_k^{\pm} = 1/(e^{-E_k^{\pm}/T} + 1). \tag{15}$$

Finally, minimizing the free energy with respect to the gap parameter W we find the gap equation

$$\frac{N_{Ta}A}{\alpha^2} = 2N_{\uparrow}(0)\int_0^{E_B}\frac{d\epsilon}{(\epsilon^2+W^2)^{1/2}}\tanh\left(\frac{(\epsilon^2+W^2)^{1/2}}{2T}\right), \tag{16}$$

where E_B is the electronic bandwidth. This gap equation is equivalent to the BCS[12] gap equation and was derived by Chan and Heine.[4] From BCS we find the transition temperature

$$k_B T_{IN} = 1.13\, E_B \exp[-N_{Ta}A/2\alpha^2 N_{\uparrow}(0)] , \tag{17}$$

the energy gap at $T = 0$,

$$2W(T=0) = 3.52\, k_B T_{IN} , \tag{18}$$

and the heat-capacity jump at T_{IN},

$$\Delta C_v = 3\times 9.4\, N_{\uparrow}(0)k_B^2 T_{IN} , \tag{19}$$

where the factor of 3 is for the 3-CDW state. The change in susceptibility is due to the opening of

the band gap and is

$$\Delta\chi \equiv \chi(T_{IN}) - \chi(0) = 1.3 \times 4\mu^2 N_\uparrow(0)\,, \tag{20}$$

including an electron-electron enhancement factor of 1.3. These results are well known and are included here for completeness.

In order to compare the model with experiment we take DiSalvo's[6] value $\Delta\chi = 55 \times 10^{-6}$ emu/mole and use (20) to find the $N_\uparrow(0) \simeq 0.33$ (states/eV Ta-atom). Using (19), the model then predicts a specific-heat jump of 0.8 (J/mol K). Craven[11] finds a specific-heat jump of 4 (J/mol K) which is a factor of 5 larger. This discrepancy is increased if the CDW interaction term is retained in the theory. The theory predicts an energy gap $2W(0) = 0.037$ eV, whereas Barker *et al.*[10] find an energy gap of 0.25 eV. These gross discrepancies force one to conclude that the "conventional theory" presented in this section is not applicable to $2H$-$TaSe_2$.

V. PHONON ENTROPY MODEL AT FINITE T

We next examine the finite-temperature theory in the opposite limit, that of small coherence length. If the coherence length is small phonon frequencies are modified over a large region of reciprocal space and the entropy of the phonons is important. If the phonon entropy is large enough, it reduces the transition temperature sufficiently that the electronic entropy is unimportant at the transition. For large coherence lengths, the energy gap at $T = 0$ is approximately $3.5\ kT_{IN}$. In order for the short coherence-length limit to apply, the energy gap at $T = 0$ must be of order $7\ kT_{IN}$. or greater. Then the electronic entropy is certainly negligible.

At low temperatures, phonons are quantized excitations. However, near the transition temperature the phonon energies are less than kT and we can use classical statistical mechanics. Equation (4) is the energy of a microscopic phase-transition model with three complex order parameters in three dimensions; the interlayer interactions are weak. It is a continuum model with a momentum space cut off. In order to calculate its properties we first transform to a discrete model and then use the mean-field approximation. On each plane we define a square lattice with lattice sites $\vec{x}_{mn}$. We define a lattice order parameter ϕ^j_{lmn} by the value of the continuum order parameter at the lattice site

$$\phi^j_{lmn} \equiv \phi^j_l(\vec{x}_{mn})\,. \tag{21}$$

We require that the number of lattice sites be equal to the number of modes in momentum space of the continuum model which gives a square lattice spacing of $\pi\xi_0$. Replacing the gradient term in (4) by the difference we find

$$E_P = \frac{1}{2}\frac{(\pi\xi_0)^2}{\Omega}\sum_{lmn}\Bigg[\sum_j\Bigg(A\,|\phi^j_{lmn}|^2 - C\,|\phi^j_{lmn}|^2 \ln\left|\frac{\phi_B}{\phi^j_{lmn}}\right|^2 + \frac{C}{\pi^2}\left(|\phi^j_{lmn} - \phi^j_{l\,m+1\,n}|^2 + |\phi^j_{lmn} - \phi^j_{l\,m\,n+1}|^2\right)\Bigg)$$
$$+ D\left(|\phi^1_{lmn}\,\phi^2_{lmn}|^2 + |\phi^2_{lmn}\,\phi^3_{lmn}|^2 + |\phi^3_{lmn}\,\phi^1_{lmn}|^2\right)\Bigg]\,. \tag{22}$$

We neglect the small terms in the energy. It may be important in a more exact calculation to retain the interlayer interaction since that term makes the problem three dimensional; within mean-field theory it is unimportant. We next transform to dimensionless quantities

$$\psi^j_{lmn} = \phi^j_{lmn}/\phi_0\,, \tag{23}$$

$$e_p = E_P[2\Omega/C(\pi\xi_0\phi_0)^2]\,, \tag{24}$$

$$t = T[2\Omega/C(\pi\xi_0\phi_0)^2]\,. \tag{25}$$

The probability of a particular configuration is

$$\exp(-E_P/T) = \exp(-e_p/t) \tag{26}$$

and

$$e_p = \sum_{lmn}\sum_j\left[\frac{A}{C} - \ln\left(\frac{\phi_B}{\phi_0}\right)^2 + (\xi_0\Delta q)^2\right]|\psi^j_{lmn}|^2 + |\psi^j_{lmn}|^2 \ln|\psi^j_{lmn}|^2 - \frac{B\phi_0}{C}\,\mathrm{Re}(\psi^{j\,3}_{lmn})$$
$$+ \frac{1}{\pi^2}\left(|\psi^j_{lmn} - \psi^j_{l\,m+1\,n}|^2 + |\psi^j_{lmn} - \psi^j_{l\,m\,n+1}|^2\right) + \frac{D\phi_0^2}{C}\left(|\psi^1_{lmn}\,\psi^2_{lmn}|^2 + |\psi^2_{lmn}\,\psi^3_{lmn}|^2 + |\psi^3_{lmn}\,\psi^1_{lmn}|^2\right)\,. \tag{27}$$

Within the mean-field approximation each mode moves in a potential

$$V_1(\psi) = \left[\frac{A}{C} - \ln\left(\frac{\phi_B}{\phi_0}\right)^2 + \frac{4}{\pi^2} + (\Delta q\,\xi_0)^2\right]|\psi|^2 + |\psi|^2 \ln|\psi|^2 - \frac{8}{\pi^2}\,\mathrm{Re}(\psi^*\langle\psi\rangle) + \frac{2D\phi_0^2}{C}|\psi|^2\langle|\psi|^2\rangle - \frac{B\phi_0}{C}\,\mathrm{Re}(\psi^3) \tag{28}$$

in the commensurate phase; in the incommensurate phase the $(\Delta q\,\xi_0)^2$ term and the cubic term are omitted. The thermal average value of a quantity is

$$\langle \Theta(\psi)\rangle \equiv \int d^2\psi\,\Theta(\psi) e^{-V_1(\psi)/t} \Big/ \int d^2\psi\, e^{-V_1(\psi)/t} \quad (29)$$

and one must solve for $\langle\psi\rangle$ and $\langle|\psi|^2\rangle$, the two order parameters, self-consistently

$$\langle\psi\rangle = \int d^2\psi\,\psi e^{-V_1(\psi)/t} \Big/ \int d^2\psi\, e^{-V_1(\psi)/t}\,, \quad (30)$$

$$\langle|\psi|^2\rangle = \int d^2\psi\,|\psi|^2 e^{-V_1(\psi)/t} \Big/ \int d^2\psi\, e^{-V_1(\psi)/t}\,. \quad (31)$$

$\langle\psi\rangle$ is the long-range order parameter and is proportional to the mean static displacement of the lattice; it vanishes in the normal phase and is finite in the incommensurate and commensurate phases. $\langle|\psi|^2\rangle$ is a short-range order parameter and is proportional to the mean-square local lattice displacement and to the mean-square local energy gap. All the parameters in (27) have been determined from the Raman-scattering experiments except $(\xi_0\Delta q)^2$. We find $(\xi_0\Delta q)^2 \simeq 0.065$ from fitting the incommensurate-commensurate transition temperature.

The thermodynamic quantities can be easily derived within mean-field theory. The energy per mode (in reduced units) is

$$E = \left[\frac{A}{C} - \ln\left(\frac{\phi_B}{\phi_0}\right)^2 + (\xi_0\Delta q)^2\right]\langle|\psi|^2\rangle + \langle\psi^2 \ln\psi^2\rangle + \frac{D\phi_0^2}{C}\langle|\psi|^2\rangle^2 - \frac{B\phi_0}{C}\langle \mathrm{Re}(\psi^3)\rangle\,, \quad (32)$$

and the classical entropy is

$$S = -\int d^2\psi\,\rho\ln\rho\,, \quad (33)$$

where

$$\rho(\psi) \equiv e^{-V_1(\psi)/t} \Big/ \int d^2\psi e^{-V_1(\psi)/t}\,. \quad (34)$$

Finally, the free energy is

$$F = E - TS = \frac{4}{\pi^2}\langle\psi\rangle^2 - \frac{D\phi_0^2}{C}\langle|\psi|^2\rangle^2 - T\ln\int d^2\psi\, e^{-V_1(\psi)/t}\,. \quad (35)$$

The self-consistency equations can be derived by minimizing the free energy with respect to the order parameters. The order parameters versus temperature are found by numerical solution of the self-consistency equations and are shown in Fig. 1. Within the approximations used here the commensurate-incommensurate transition is first order and the incommensurate-normal metal transition is second order. Note that the rms local energy gap [which is proportional to $(\langle|\psi^2|\rangle)^{1/2}$] drops to 86% of its zero-temperature value at the onset transition and then increases slowly. This is in marked contrast to the large coherence-length model where the energy gap vanishes at the onset transition. The entropy jump at the commensurate-incommensurate transition is $0.10\,k_B$ and the heat-capacity jump at the onset transition is $1.67\,k_B$. The dimensionless transition temperature is 0.296.

We can also calculate the temperature dependence of the phonon frequencies within the mean-field approximation and using the adiabatic approximation ($\omega\tau \ll 1$, where τ is the longest relaxation time in the system). The elastic constant appropriate to the symmetric amplitude mode [the A_{1g} mode of equation (10a)] at Γ is proportional to $\partial^2 F/\partial\langle\psi\rangle^2$ and the computed temperature dependence of the A_{1g} mode is shown in Fig. 2. The mode frequency agrees with the Raman measurement at low temperature since the model parameters were determined by fitting the Raman frequencies. At room temperature, the computed frequency agrees fairly well with Moncton's neutron data. At 125 K just above the phase transition, Moncton's data show a peak of reduced intensity at 4.5 meV; resolution effects complicate this measurement and it is suspected that the real frequencies are somewhat lower. However, the mode does not appear to go totally soft at the phase transition as predicted by the mean-field theory. It appears that the adiabatic approximation has broken down due to critical slowing down near the phase transition.

We now test the short coherence-length model by comparing it with experiment. We can extract two

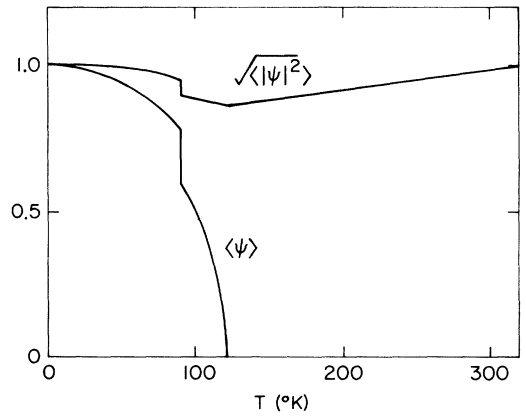

FIG. 1. Long-range order parameter $\langle\psi\rangle$ and the square root of the short-range order parameter $\langle|\psi|^2\rangle$ vs temperature according to the short coherence-length theoretical model.

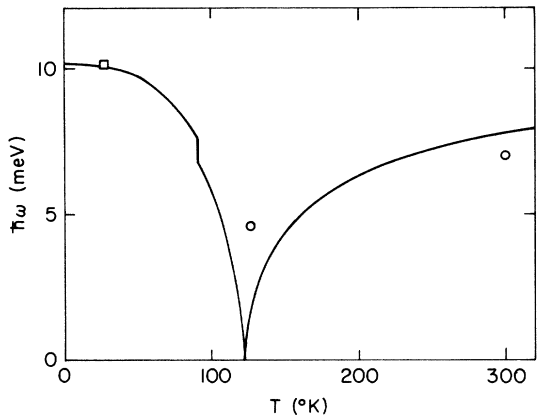

FIG. 2. Solid curve is the calculated phonon energy of the symmetric amplitude (A_{1g}) mode vs temperature. The open square is from the Raman data of Holy *et al.* and the open circles are from the neutron data of Moncton *et al.*

parameters from the experimental transition temperature and heat-capacity jump. Craven's heat-capacity jump is $\simeq 4$(J/(mol °K) which is $0.48k_B$ per Ta atom. With $\Delta C = 1.67k_B$ per mode we find three modes per ten Ta atoms or three modes per superlattice unit-cell area. The correlation length is therefore about $\pi\xi_0 \simeq 10$ Å which is equal to the super-lattice unit-cell length which is as short as is physically reasonable for a correlation length. We can confirm this magnitude of the correlation length by comparing with other data. Moncton has measured the ratio of the basal-plane correlation length (actually the longitudinal one in the $\vec{q}$ direction) to the c-direction correlation length and finds a ratio of 3. Within mean-field theory, that ratio is $[C\xi_0^2/F\frac{1}{2}c^2]^{1/2} = 2.0$ which is satisfactory agreement since we have neglected the anisotropy of the basal-plane correlation length. The extent in k space of the Kohn anomaly should be $\simeq 1/\xi_0 = 0.12(4\pi/\sqrt{3}a)$ which agrees with the extent of the anomaly observed in the $\Sigma_1[100]$ longitudinal-acoustic-phonon branch of $2H$-$TaSe_2$ by Moncton and Axe. Thus, the short coherence length is consistent with several experiments and it is clear that $2H$-$TaSe_2$ is in the short coherence-length limit. The computed transition temperature is

$$T_{IN} = 0.296\, C(\pi\xi_0\phi_0)^2/2\Omega\ . \qquad (36)$$

With $T_{IN} = 122$ K, $C = 0.29$ eV/Å, and $(\pi\xi_0)^2/\Omega = 10$, we find $\phi_0 \simeq 0.16$ Å. Moncton has measured ϕ_0 directly using neutron crystallographic techniques and finds ϕ_0 between 0.05 and 0.09 Å which provides another experimental test of the model.

With such a short coherence length, the energy gap is the same order of magnitude as the Fermi energy. We can obtain a rough order-of-magnitude estimate of the energy gap as follows. From Mattheiss's[13] band structure (for $2H$-TaS_2) the Fermi energy is 0.35 eV and the (isotropically averaged) basal-plane band mass is about 5 electron masses. Using $\xi_0 \simeq \hbar v_F/2W$ we estimate $2W_0 \simeq 0.3$ eV which is in order-of-magnitude agreement with the weak absorption edge (at 0.25 eV) observed in infrared reflectivity by Barker *et al.* The observed energy gap of $24\, k_B T_{IN}$ fits in nicely with the short coherence-length model but is inconsistent with the long coherence-length model.

The short coherence-length model works very well in a semiquantitative way in comparing orders of magnitude of quantities. Since Moncton and Axe have measured the temperature dependence of the long-ranged order parameter in $2H$-$TaSe_2$ we can have a detailed quantitative test of the model (within the mean field approximation). This comparison is shown in Fig. 3. The model is not in quantitative agreement with the measured order parameter, particularly near the onset transition. The deviation is in the direction expected from the effects of critical fluctuations with the measured order parameter rising more rapidly (smaller exponent) and to a larger value than the computed order parameter. With a short coherence length one expects strong critical behavior and this behavior is clearly present in Craven's heat-capacity data. Thus the mean-field approximation is at least partly to blame for the disagreement in Fig. 3. Since the mean-field theory is not quantitative the estimates of ξ_0 and ϕ_0 are accurate only within ± 50%. The drop in order parameter at the commensurate-incommensurate transition (at 90 K) is several times smaller than predicted. At least part of the reason for this discrepancy is the fact that amplitude and phase distortions of the or-

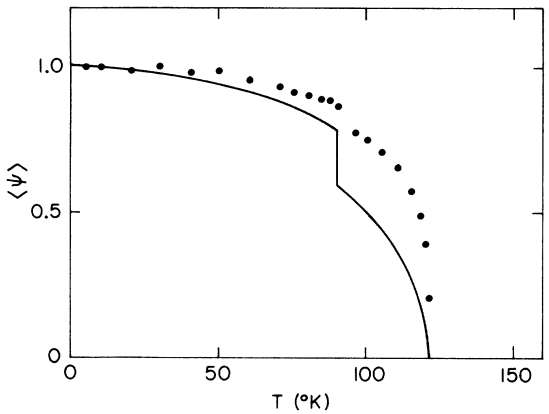

FIG. 3. Comparison of the long-range order parameter of the theoretical model (solid curve) with the square root of the superlattice Bragg scattering intensity from Moncton *et al.*

der parameter, which are known to be present in the incommensurate phase,[8,14] have been left out of the present theory. The dynamical behavior near the phase transition is also poorly predicted by the mean-field calculation. Since all these discrepancies may be due to defects in the mean-field approximation rather than defects in the physical model, it is very important to have more quantitative calculations based on the physical model.

The physical picture of charge-density waves in $2H$-$TaSe_2$ which we have arrived at is as follows. The CDW modes in different superlattice unit cells can be treated as independent local modes with intercell interactions. In each superlattice unit cell, each mode consists of a localized longitudinal phonon together with a localized electronic energy gap. The phonon mode has both amplitude and phase, and at low temperature, there is long-range phase coherence of the phonon modes and one has a uniform periodic lattice distortion and a constant energy gap. At the phase transition, the long-range phase coherence breaks up and the long-range order parameter goes to zero. However, there is still a large amplitude of the local phonon mode in one superlattice unit cell and a large but fluctuating local energy gap. The temperature dependence of the long-range order parameter $\langle\psi\rangle$ and of the local rms energy gap are shown in Fig. 1. The rms energy gap is quite large at the phase transition and increases with increasing or decreasing temperature. Fluctuations of the energy gap will be strong near the phase transition and at higher temperature and will smear the gap structure observed in an optical experiment. These fluctuations should also cause strong electron scattering at high frequency. Within this model the decrease in susceptibility observed at the phase transition is due to the increased area of Fermi surface eclipsed by the CDW as the rms energy gap grows.

VI. CHARGE-DENSITY WAVES AND CHEMICAL BONDING

The chemical bond in organic or solid-state systems has long been described as intermediate between the ionic bond and the covalent bond.[15,16] Both limiting cases can be understood in simple terms. The metallic bond has not found its place in chemical dogma. I would like to suggest that the CDW concept forms the natural link between the metallic bond and the ionic-covalent bond. It may be a very useful concept in narrow band-gap materials.

We start with a metal and consider opening a CDW energy gap in the band structure. In order to gain the most energy, the $\vec{q}$ vector of the CDW must span nested portions of the Fermi surface. When the gap is small the correlation length is quite long; if one wants to use a chemical-bond concept one must consider a very delocalized bond covering many metal atoms. Also, the directiveness of the bond is determined by the nature of the Fermi surface, not by the configuration of neighboring atoms. For a larger energy gap, comparable to the Fermi energy or bandwidth, the coherence length is short and the chemical bond is much more localized. In addition the atomic displacements are larger and the nonlinear terms in the electron-lattice interaction become important; the energy gap is maximized (and total energy minimized) if the pattern of atomic displacements minimizes bond lengths between pairs of atoms. These nonlinear terms pick out a bonding displacement pattern and cause the CDW's to lock into the lattice. Thus, one begins to pick up the directional character of the chemical bond in this intermediate strength case with the energy gap of the same order as the Fermi energy. The pair-bonding pattern is clearly seen in the displacement pattern for $2H$-$TaSe_2$ in Fig. 4. Finally for energy gaps much larger than the bandwidth, the metallic character disappears and one approaches the conventional ionic-covalent picture with bond directiveness controlled by the spatial character of the local atomic orbitals.

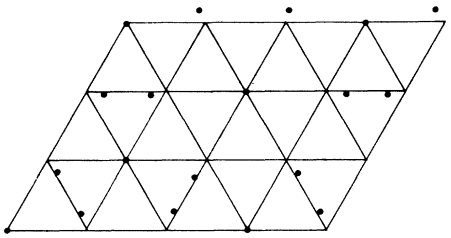

FIG. 4. Ta atomic displacement pattern in the commensurate phase of $2H$-$TaSe_2$ taken from the data of Moncton *et al.* and Holy *et al.* The displacements are exaggerated for clarity and show the pairing of six of the nine atoms in the superlattice unit cell.

VII. CONCLUSIONS

A theoretical model of charge-density waves in $2H$-$TaSe_2$ has been proposed which is in semiquantitative agreement with the available experimental data. Quantitative agreement is still lacking and further theoretical work is indicated. We have shown the short coherence-length limit is applicable to $2H$-$TaSe_2$ and it follows that this limit is applicable to the homologous materials $2H$-$NbSe_2$ and $2H$-TaS_2. It appears likely that this

limit is applicable to other CDW materials with low onset temperatures; however, one should be cautious in applying this model to other materials before sufficient experimental data is available to test the model.

ACKNOWLEDGMENTS

The author would like to thank Miles Klein and Bob Craven for helpful discussions and for making their data available prior to publication.

---

†Supported in part by NSF Grant No. DMR75-20376.

[1]R. E. Peierls, *Quantum Theory of Solids* (Clarendon, Oxford, 1955).
[2]H. Fröhlich, Proc. R. Soc. Lond. A 223, 296 (1954).
[3]A. W. Overhauser, Phys. Rev. 167, 691 (1968); Phys. Rev. B 3, 3173 (1971).
[4]S.-K. Chan and V. Heine, J. Phys. F 3, 795 (1973).
[5]F. Denoyer, R. Comés, A. F. Garito, and A. J. Heeger, Phys. Rev. Lett. 35, 445 (1975).
[6]J. A. Wilson, F. J. DiSalvo, and F. Mahajan, Adv. Phys. 24, 117 (1975).
[7]Griff Bilbro and W. L. McMillan, Phys. Rev. B (to be published).
[8]D. E. Moncton, J. D. Axe, and F. J. DiSalvo, Phys. Rev. Lett. 34, 734 (1975); D. E. Moncton, Ph.D. thesis (MIT, 1975) (unpublished).
[9]J. A. Holy, M. V. Klein, W. L. McMillan, and S. F. Meyer (unpublished).
[10]A. S. Barker, Jr., J. A. Ditzenberger, and F. J. DiSalvo (unpublished).
[11]R. Craven (unpublished).
[12]J. Bardeen, L. N. Cooper, and J. R. Schrieffer, Phys. Rev. 108, 1175 (1957).
[13]L. F. Mattheiss, Phys. Rev. B 8, 3719 (1973).
[14]W. L. McMillan, Phys. Rev. B (to be published).
[15]Linus Pauling, *The Nature of the Chemical Bond* (Cornell U.P., Ithaca, N. Y. 1939).
[16]J. C. Phillips, Rev. Mod. Phys. 42, 317 (1970).